

1 **THIS IS AN EARTHARXIV PREPRINT OF AN ARTICLE SUBMITTED FOR**
2 **PUBLICATION TO THE ANNALS OF GLACIOLOGY**

3 **Basal melt over Subglacial Lake Ellsworth and its catchment: insights from englacial layering**

4 **Ross, N.¹, Siegert, M.²,**

5 **¹School of Geography, Politics and Sociology, Newcastle University, Newcastle upon Tyne,**

6 **UK**

7 **²Grantham Institute, Imperial College London, London, UK**

Basal melting over Subglacial Lake Ellsworth and its catchment: insights from englacial layering

Neil ROSS,¹ Martin SIEGERT,²

¹*School of Geography, Politics and Sociology, Newcastle University, Newcastle upon Tyne, UK*

²*Grantham Institute, Imperial College London, London, UK*

Correspondence: Neil Ross <neil.ross@ncl.ac.uk>

ABSTRACT. Deep-water ‘stable’ subglacial lakes likely contain microbial life adapted in isolation to extreme environmental conditions. How water is supplied into a subglacial lake, and how water outflows, is important for understanding these conditions. Isochronal radio-echo layers have been used to infer where melting occurs above Lake Vostok and Lake Concordia in East Antarctica but have not been used more widely. We examine englacial layers above and around Lake Ellsworth, West Antarctica, to establish where the ice sheet is ‘drawn down’ towards the bed and, thus, experiences melting. Layer drawdown is focused over and around the NW parts of the lake as ice, flowing obliquely to the lake axis, becomes afloat. Drawdown can be explained by a combination of basal melting and the Weertman effect, at the transition from grounded to floating ice. We evaluate the importance of these processes on englacial layering over Lake Ellsworth and discuss implications for water circulation and sediment deposition. We report evidence of a second subglacial lake near the head of the hydrological catchment and present a new high-resolution bed DEM and hydropotential model of the lake outlet zone. These observations provide insight into the connectivity between Lake Ellsworth and the wider subglacial hydrological system.

32 INTRODUCTION

33 The exploration, access and measurement of Antarctic subglacial lakes has the potential to address several
34 significant scientific questions regarding Antarctic Ice Sheet history, life in extreme environments, and how
35 subglacial hydrology can influence ice sheet flow (Siegert, 2016). Important to each of these questions is
36 how water is supplied to, and released from, subglacial lakes. Considerable focus has been given to inputs
37 and outputs associated with water flow across the ice sheet bed (e.g. Wingham and others, 2006; Fricker
38 and others, 2007; Wright and others, 2012; Fricker and others, 2016) but there has been relatively little
39 investigation constraining basal melt of the overlying ice sheet at the ice-water interface. A characteristic
40 of the ice sheet that can be exploited to constrain both the location and magnitude of basal melting is
41 the englacial structure of the ice sheet, which can be imaged and characterised using radio-echo sounding
42 (RES) (Siegert, 1999; Dowdeswell and Evans, 2004). Englacial layers, associated with variations in the
43 density, conductivity and crystal fabric of the ice sheet, are assumed to be isochronous and, in most
44 cases, are associated with the burial of palaeo-ice sheet surfaces (Siegert, 1999). Over subglacial water
45 bodies, and localised areas of high geothermal heat flux, englacial layers can be locally drawn down so that
46 younger layers are found at greater than expected depths in the ice sheet column, indicative of high rates
47 of subglacial melt (Siegert and others, 2000; Gudlaugsson and others 2016; Jordan and others, 2018).

48 Direct melting of the overlying ice sheet into subglacial lakes influences: (i) the pattern and rate
49 of circulation of the water body (Thoma and others 2009, 2011; Woodward and others, 2010), through
50 determining where water is introduced to the lake; and (ii) subglacial lacustrine sedimentary processes
51 (Bentley and others, 2011; Smith and others, 2018), by influencing where sediments melt out from the
52 overlying ice and be deposited on the lake floor. Whilst basal melting at the ice-water interface does not
53 operate in isolation, i.e. in an open system it will interact with subglacial water flowing between the ice
54 sheet and the bed, improved knowledge of its location and magnitude will enhance the understanding of
55 the drivers of hydrological processes in subglacial lakes.

56 Numerical modelling of water circulation has been undertaken for three Antarctic subglacial lakes
57 (Pattyn and others, 2016): Lake Vostok (e.g. Wüest and Carmack, 2000; Mayer and others, 2003; Thoma
58 and others 2008a, 2008b), Lake Concordia (Thoma and others, 2009) and Subglacial Lake Ellsworth (SLE)
59 (Woodward and others, 2010; Thoma and others, 2011). The most up-to-date water circulation model
60 applied to subglacial lakes, ROMBAX, is an adapted 3D ocean model. This model integrates hydrodynamic

61 equations, the geometry of the water body, and a formulation to estimate the mass balance (i.e. rates of
62 melt and refreezing) at the ice–lake interface (Pattyn and others, 2016). ROMBAX assumes that the lake
63 system is closed (i.e. no lake inflow or outflow). Inclined ice-water interfaces that induce melting in deeper
64 areas and refreezing in higher areas generate water circulation in subglacial lakes. Well-constrained lake
65 geometries are therefore essential for determining the basal mass balance. With constraint on ice flow, the
66 thickness and distribution of accretion ice can be calculated (Woodward and others, 2010). Input data
67 for ROMBAX modelling of Lake Vostok, Lake Concordia and SLE comprise lake bathymetry (i.e. water
68 column thickness) determined from seismic reflection surveys or the inversion of gravity measurements,
69 ice thickness, assumed values of geothermal heatflux and the velocity of ice flow from GPS or InSAR
70 measurements. For each lake a basal mass balance (i.e. a prediction of where basal melt, causing layer
71 drawdown, and refreezing, causing layer uplift, occurs), the pattern and velocity of water flow, and the
72 extent and thickness of accreted ice, have been determined. In comparison to Lakes Concordia and Vostok,
73 water circulation modelling suggests that SLE has higher rates of basal melt, basal refreezing and a more
74 vigorous water circulation (see: Table 1 of Pattyn and others, 2016). In addition, SLE is positioned at
75 a depth that intersects the Line of Maximum Density (Wüest and Carmack, 2000; Thoma and others,
76 2011); a critical pressure depth (3050 m) between dense water that will sink when warmed (ice overburden
77 pressure < critical water pressure) and water that is buoyant and will rise when warmed (ice overburden
78 pressure > critical water pressure). The physical consequences of this in SLE are that deeper parts of
79 the lake may experience convective (ocean-type) circulation leading to mixing of the water column, whilst
80 shallower parts may have limited convection and a stratified water column (Woodward and others, 2010;
81 Thoma and others, 2011; Pattyn and others, 2016). However, the vigorous water circulation induced by
82 the steep ice-water interface at SLE, means that water circulation, and hence mixing of the water column,
83 may occur irrespective of the critical pressure boundary (Woodward and others, 2010; Thoma and others,
84 2011).

85 The aims of this paper are to report the character and 3D form of the englacial layer package over
86 SLE and its wider catchment, to: (i) identify and explain the processes responsible for layer morphology;
87 (ii) assess whether the geometry of the englacial layers is spatially consistent with output from existing
88 numerical models of water circulation in SLE; (iii) improve understanding of the interactions between SLE
89 and the overlying ice sheet (i.e. identifying potential sources of meltwater); (iv) analyse catchment-scale
90 hydrological connectivity; and (v) evaluate conceptual models of sediment deposition in SLE. Our study is

91 justified by the surprisingly few detailed observational investigations (3D or otherwise) of englacial layers
92 over and around subglacial lakes (see: Siegert and others, 2000; Leonard and others, 2004; Siegert and
93 others, 2004; Tikku and others, 2005; Carter and others, 2009), the unparalleled resolution, detail and
94 tailored survey design of the SLE RES dataset, and the forthcoming exploration of Subglacial Lago CECs
95 (Rivera and others, 2015), located not far from SLE, by a UK-Chilean research programme.

96 **SUBGLACIAL LAKE ELLSWORTH**

97 Between 2007-09 SLE was subject to a comprehensive ground-based geophysical characterisation, including
98 RES, seismic reflection, GPS and shallow ice core measurements, and numerical modelling of water circu-
99 lation patterns, in advance of an attempt at direct access and exploration in 2012 (Woodward and others,
100 2010; Ross and others, 2011a; Siegert and others 2012, 2014; Smith and others 2018). Whilst the basal
101 topography, water column thickness, nature of the sediments on the lake floor and the catchment-scale
102 subglacial hydrological flow paths have been constrained and published (Ross and others, 2011a; Siegert
103 and others 2012; Smith and others, 2018), few details of the englacial layer form have been reported. Ross
104 and others (2011b) reconstructed Holocene ice flow using englacial layer folding, but did not report or
105 discuss the implications of the broader internal layer geometry for SLE. Here, we describe the RES survey
106 of SLE, detailing the geometry and character of englacial layers in the SLE RES dataset. This is the first
107 time that this dataset has been reported and described. We also present a high-resolution digital elevation
108 model (DEM) of the outlet area of SLE.

109 **METHODS**

110 The RES survey used the ground-based ~ 1.7 MHz pulsed DEep-LOOk-Radar-Echo-Sounder (DELORES)
111 RES system (King and others, 2016) towed by a snow mobile at an average rate of ~ 12 km hr⁻¹. Traces,
112 comprising the stacking of 1000 measurements, were acquired at an approximate along-track sampling
113 resolution of 3-4 m. The survey (Figure 1a) was designed to characterise the physical system of the
114 subglacial environment, from the ice divide to beyond the down-ice end of SLE, as well as the extent and
115 form of the lake surface. A nested grid of closely-spaced (i.e. line-spacing of 300-350 m) RES lines were
116 acquired at the down-flow end of the lake, with the aim of characterising the bed topography in high-
117 resolution to measure any outlets of water and associated morphology. Nearly 1000 km of RES data were
118 acquired, with the ice-bed identified and picked in more than 95% of the data (Ross and others, 2011a).

119 Post-processing of the RES data in the software Reflexw comprised a typical processing scheme for low
120 frequency impulse RES data (i.e. bandpass frequency filter, gain to compensate for geometrical divergence
121 losses, Kirchhoff migration). Processed data were displayed, and picked layers assigned to ice thickness
122 values, assuming a radio-wave velocity of 0.168 m ns^{-1} . A series of eight englacial layers were identified
123 and picked; the uppermost seven of these layers could be traced continuously over a wide region allowing
124 them to be gridded. Picking of layers was not possible, or was not continuous, where high-amplitude layer
125 buckles, steep layer slopes and/or offline reflectors occurred. DEMs were generated from the layer picks
126 using the topo2raster algorithm (Hutchinson, 1988). Picks of the ice thickness and subglacial topography
127 from the DELORES surveys, combined with existing ground and airborne RES surveys (e.g. Vaughan
128 and others, 2007), were also gridded using the topo2raster algorithm to produce a DEM of the glacier bed
129 (Figures 1c and 5b). The grid, combined with ice surface elevation (see below), was used to calculate the
130 hypopotential of the outlet zone of SLE (Figure 5c), following the methods detailed in Jeofry and others
131 (2018). The extent of SLE (Figure 1) was determined from the identification of a qualitatively bright
132 smooth specular radar reflection at the base of the trough. Ice surface elevation was measured along the
133 RES profile lines with Leica (500 and 1200) GPS in rover mode, with processed observations gridded to
134 generate a DEM of the ice surface. A horizontal offset between the GPS (on lead skidoo) and the midpoint
135 of the radar antennas was corrected manually during post-processing. Four static Leica GPS base stations
136 (three over the lake, one on slow flowing ice adjacent to it) were used to measure ice flow velocity (Figure
137 1b) and any possible vertical displacement during the 2007-08 field season (Woodward and others, 2010),
138 and to correct the position of the roving data. Two static Leica base stations were used in the 2008-09
139 season (one over the lake, one on slow flowing ice adjacent to it). A network of stakes were used to provide
140 more extensive ice flow constraints (Figure 1b) (Ross and others, 2011b).

141 RESULTS

142 The RES stratigraphy across the survey area is characterised by a series of strong, bright, thick, discrete
143 reflections to depths up to 2500 m below the ice surface (Figure 2). In large parts of the survey area (Figure
144 1a), including areas below the ice divide, few if any layers are observed in the radargrams at depths greater
145 than 2500 m, suggesting a thick (up to 1 km in places) echo-free zone (Drewry and Meldrum, 1978). The
146 englacial reflections are typically continuous, although one or two layers (e.g. between picked layers 2 and
147 3) demonstrate bifurcation and pinch-out when ice thickness increases and decreases, respectively (Figure

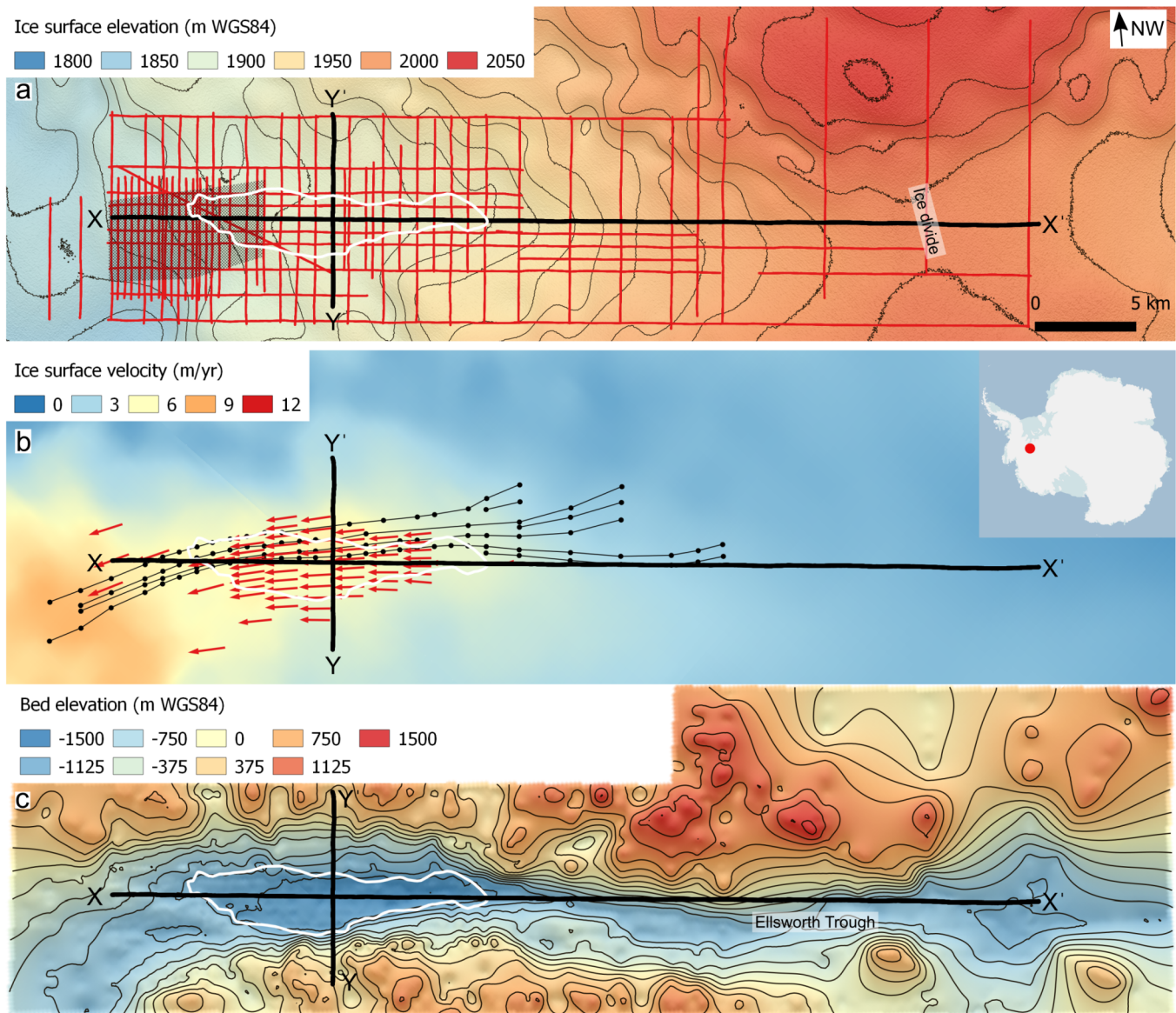


Fig. 1. Location of Subglacial Lake Ellsworth (SLE), West Antarctica: (a) Ice surface topography (m WGS84) from Reference Elevation Model of Antarctica (REMA) (Howat and others, 2019), underlain by a hillshade of the same data (illuminated from azimuth of 315° and altitude of 30° , with Z factor of 100). Contours in 10 m intervals. The red lines are the location of SLE DELORES ice-penetrating radar data. The hatched area represents the extent of Figures 5b and 5c. The locations of the radargrams in Figure 2 are shown as black lines; (b) Ice flow velocity from MEaSURES (Mouginot and others, 2019), overlain by GPS measurements of ice flow (red arrows) and orientation of internal layer folds (black dots and thin black lines) (from Ross and others, 2011b). The locations of the radargrams in Figure 2 are shown as thick black lines. The inset shows the location of SLE in Antarctica; (c) Subglacial topography (m WGS84) of the Ellsworth Trough (from Ross et al., 2011a; Ross and others, 2014). Basal topography over SLE is the lake ice-water interface, not the lake floor. Contours in 200 m intervals. The locations of the radargrams in Figure 2 are shown as black lines. Figures 1a-c are rotated clockwise by 41.4° . The extent of SLE is shown by white polygons.

148 2). A prominent feature of the RES data over SLE are buckles generated by up-ice flow over rugged
149 subglacial topography (Ross and others, 2011b), which disrupt the layer stratigraphy and geometry, and
150 limit uninterrupted layer picking in ice >500 m below the ice surface in some areas (Figures 1b, 2c and
151 2d). The thickness of the englacial reflections (~ 10 m) is consistent with them representing the merged
152 radar-response of multiple thinner discrete layers (Siegert, 1999; Dowdeswell and Evans, 2004).

153 Across ice flow, englacial reflections drape over the rugged topography with traceable layers over the
154 Ellsworth Trough mapped at ice thicknesses up to double that observed over the topographic highs of the
155 valley sidewalls and surrounding highlands and interfluves (Figures 2 and 3). This layer relief (i.e. of up
156 to 1000 m) results in steep englacial layer slopes, which may account for the loss of returned radio-wave
157 power off some of the deeper layers (e.g. layer 8) proximal to the trough's main side walls (Figure 2c).

158 It is apparent from both the radargrams and the gridded DEMs that subglacial topographic relief may
159 not be the only factor influencing englacial form and geometry, however. The maximum drawdown of
160 layers is offset from the centre of the trough axis, with drawdown focused NW of the trough's long axis
161 (e.g. right-hand side of Figure 2a and 2c). In gridded layers 2-7 the axis of maximum drawdown has a
162 spatial correspondence with the mapped NW lateral edge (i.e. shoreline) of the lake and the NW half of
163 the lake (Figure 3). This is in direct contrast to the geometry of these layers over the SE side of the lake,
164 where the elevation of all these layers is observed to be rising in the ice located above the lake shoreline
165 (Figure 2a, 2c and 3). As such, maximum drawdown is offset to the NW of the central axes of both the
166 Ellsworth Trough and SLE.

167 Although there is some sagging of layers throughout the Ellsworth Trough, drawdown is much more
168 pronounced along the length of the lake (Figure 2b and 3). In the deeper layers (i.e. layer 4 and below)
169 a second zone of enhanced drawdown is apparent in the base of the Ellsworth Trough between SLE and
170 the ice divide (Figure 3e-h). RES data perpendicular to this zone of layer drawdown are associated with a
171 localised qualitatively bright flat basal reflection in the deepest part of the trough, where the ice is thick
172 (Figure 3a), directly beneath the maximum layer drawdown (Figure 4). This is indicative of the presence of
173 a smaller water body in the Ellsworth Trough between SLE and the ice divide (Figure 4), and is consistent
174 with the potential for a connected subglacial hydrological system along the base of the Ellsworth Trough
175 (Vaughan and others, 2007; Siegert and others, 2012; Smith and others, 2018; Napoleoni and others, in
176 prep).

177 Down-ice of SLE, the englacial layers rise in elevation as the bed rises, and ice flows over a prominent

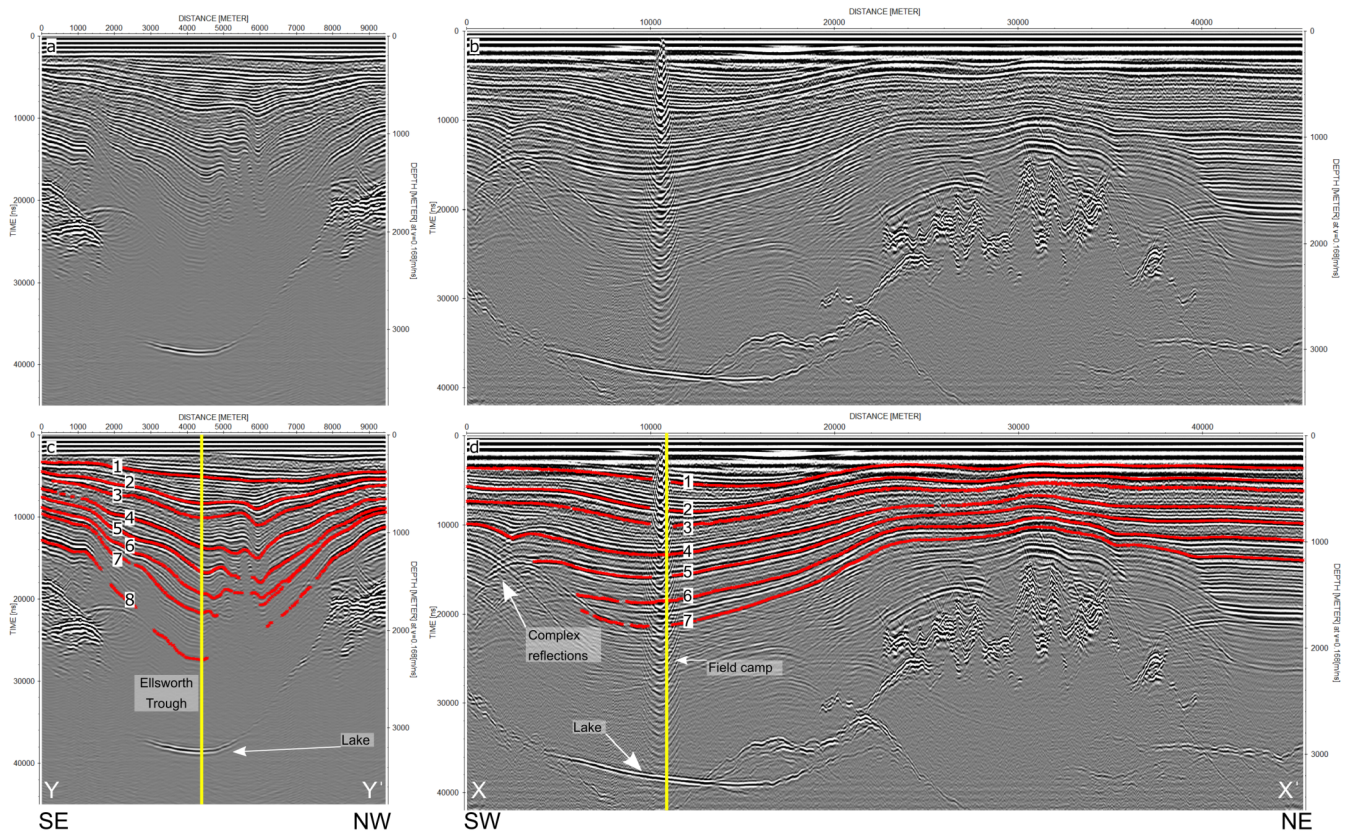


Fig. 2. Example radargrams of RES data and the eight picked layers (1-8) over Subglacial Lake Ellsworth (SLE) and surroundings: (a) Radargram from survey line D7.5 acquired across SLE, just up ice of its centre point. Ice flow is into page with a slight convergence of flow (Figure 1b). (b) Radargram from survey line C5, acquired from just across the ice divide along the long axis of the Ellsworth Trough and SLE. Ice flow is approximately right to left, although with a slightly oblique component particularly close to X (see Figure 1b). Note that the apparent subglacial mountain range between 20-40 km is an offline reflection due to proximity of rugged relief. (c) as 2a, but with eight picked englacial layers shown (red lines); (d) as 2b, but with seven picked englacial layers shown (red lines). Complex reflections from a series of buckled layers intersecting obliquely with the survey line (see Figure 1b) and the 2007/08 field camp are indicated. Only seven layers were pickable in line C5, as layer 8 was not readily identifiable in this orientation. Yellow lines show intersection point of radargrams. Location of transects is shown in Figure 1a-c.

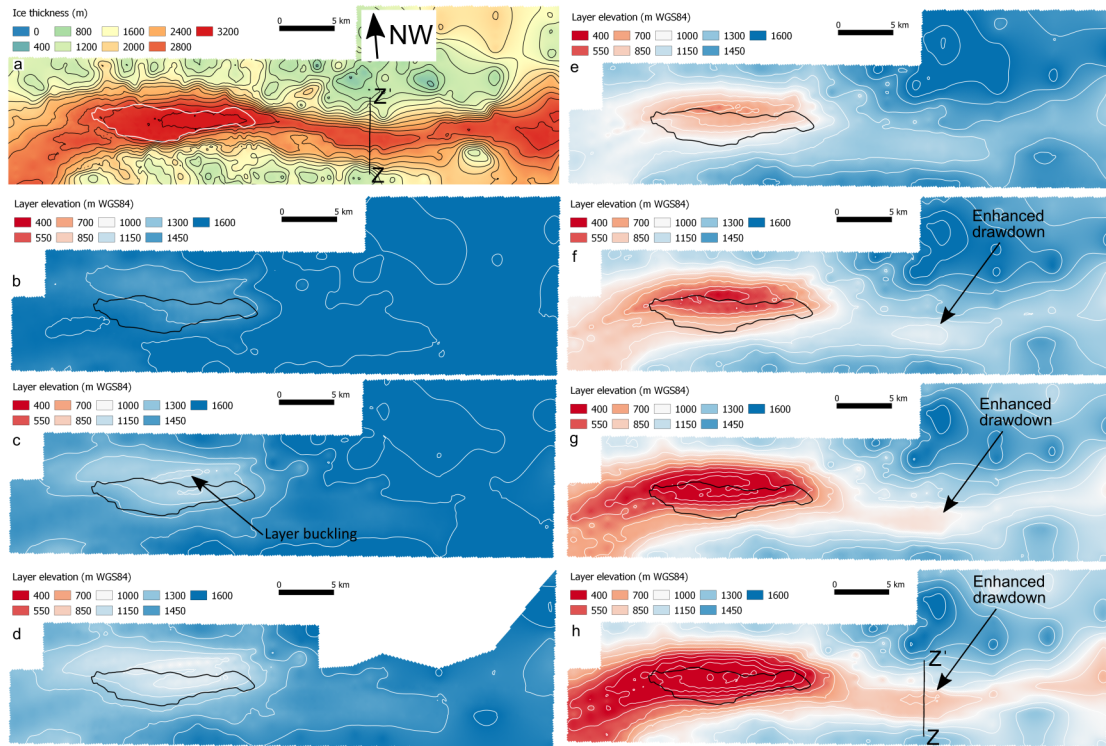


Fig. 3. Elevation (m WGS84) of gridded englacial layers 1-7 throughout the SLE catchment. (a) ice thickness (m) (from Ross et al., 2011a) with contours at 200 m intervals. Location of RES line D18.25 (Figure 4a) is shown by a black line; (b) layer 1 elevation; (c) layer 2 elevation; (d) layer 3 elevation; (e) layer 4 elevation; (f) layer 5 elevation; (g) layer 6 elevation; (h) layer 7 elevation. Location of RES line D18.25 (Figure 4) is shown by a black line. All layers are shown with a common colour scale that is saturated below 400 m WGS84 and above 1600 m WGS84, to demonstrate their evolution with depth through the ice column. All layer elevation contours are at 100 m intervals. The lake shoreline is represented by white (a) and black (b-h) polygons. The orientation of Figures 3a-h have been rotated clockwise by 41.4° for display.

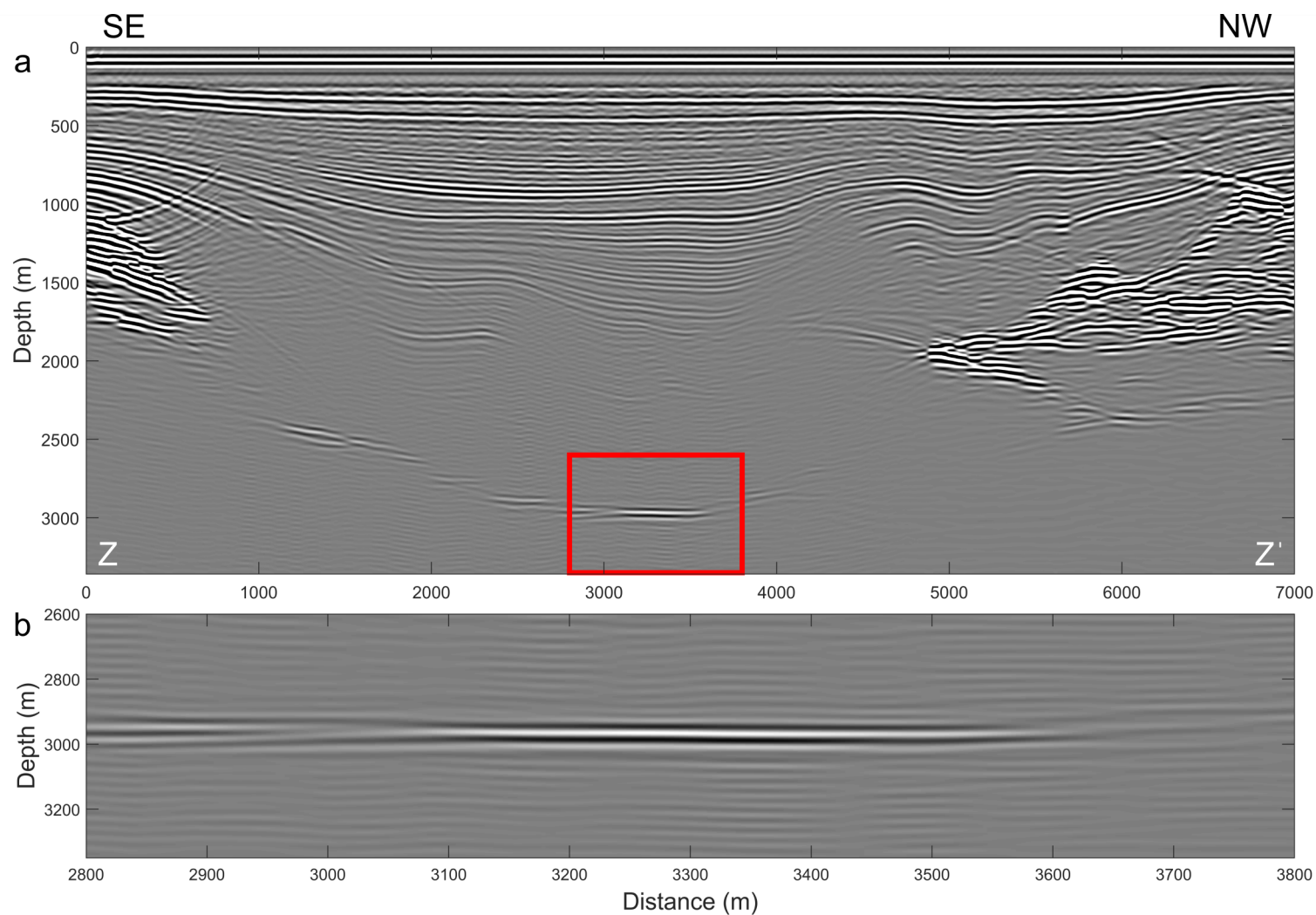


Fig. 4. Engacial layer geometry and basal reflection properties associated with a small subglacial water body in the upper Ellsworth Trough. (a) Radargram from survey line D18-25 showing bed topography and englacial layers (see figures 3a and 3h for location). The red box shows the extent of Fig. 4b; (b) zoom-in of radargram D18.25 showing the qualitatively bright flat specular reflection on the floor of the Ellsworth Trough at an ice thickness of nearly 3 km.

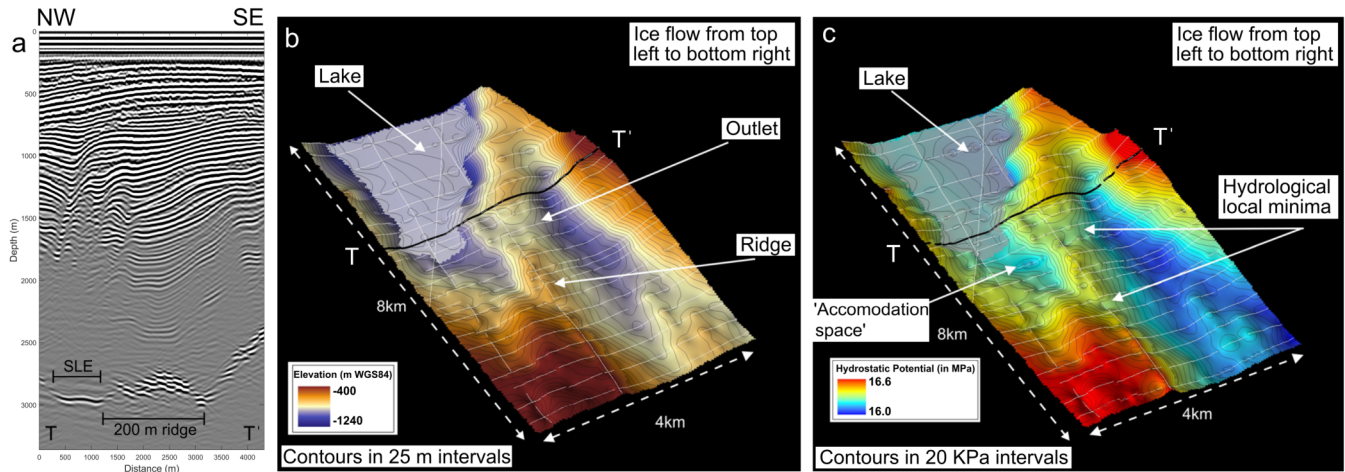


Fig. 5. High resolution topography and hydropotential of the outlet zone of SLE. (a) Radargram E2 (for location see 5b and 5c) displaying a narrow bright reflection from the down-ice most part of SLE, and the subglacial topography, including a 200 m high ridge that impounds the down-ice end of the lake; (b) RES-derived DEM of the topography at the outlet of SLE. The lake, its downstream ridge and possible lake outlets are annotated; (c) RES-derived hydropotential map of the outlet zone of SLE, showing the hydropotential high associated with the subglacial ridge. Potential hydrological lows, where water may discharge from SLE, are shown. White lines on 5b and 5c are the location of all DELORES RES data used to produce the topography DEM and the derived hydropotential map. The location of radargram E2 (5a) is represented by a black line. DEM horizontal cell size for 5b and 5c is 50 m. The extents of 5b and 5c are shown in Figure 1a.

178 ridge that impounds the bottom end of the lake (Figure 5) (Siegert and others, 2012; Ross and others,
179 2014; Smith and others, 2018). The layer form is also consistent with a transition from sliding to no-sliding
180 associated with the down-ice lake shoreline (Weertman, 1976; Leysinger Vieli and others, 2007). In these
181 'down-ice' parts of the survey area (i.e. SW) englacial reflections are observed nearer to the (on average
182 slightly shallower) bed, with a thinner echo-free zone (Figure 5a). No evidence for englacial reflections
183 associated with accretion ice (Bell and others, 2002) have been observed in any of the DELORES data
184 over and around SLE. The detailed geomorphology of the SLE outlet zone is presented here for the first
185 time (Figure 5b) and reveals a clear relationship between the 200 m high basal ridge that trends obliquely
186 across the valley, and the down-ice shoreline of SLE. The DEM and hydropotential analysis (Figures 5b
187 and 5c) also reveals that, down-ice of the ridge, there is a second smaller basin, and hydropotential low,
188 between the ridge and the SE valley wall. Two possible hydrological connections, associated with low-lying
189 channels that appear to cut across the ridge (Figures 5b and 5c), may connect SLE with this basin during
190 lake highstands associated with either periods of enhanced basal melt, or changes in the steepness of the
191 ice surface (Siegert, 2005). 15-20 km beyond SLE another large subglacial lake has been observed with
192 airborne RES (Vaughan and others, 2007; Napoleoni and others, in prep), and it is possible that episodic
193 connection between SLE and this down-ice lake occurs during such highstands.

194 DISCUSSION

195 We have demonstrated that englacial layer drawdown over SLE is focused on the lateral NW shoreline and
196 NW half of the lake. This initially appears to be a surprising finding as, intuitively, we would anticipate
197 basal melting, and therefore englacial layer drawdown, to be focused at the up-ice end of any subglacial
198 lake, where the ice is thickest, and the ice-water interface is lowest. However, processes other than basal
199 melting, such as the Weertman effect (Weertman, 1976; Barcilon and MacAyeal, 1993; Leysinger-Vieli and
200 others, 2007) may also play a role in controlling englacial layer form in this case.

201 GPS observations show that ice flow (Fig. 1b) is slightly oblique to the axis of the Ellsworth Trough
202 (Ross and others, 2011b). This means that the ice does not flow straight down the trough, but instead
203 flows north of NE to south of SW (i.e. obliquely across the trough and the lake). When combined with the
204 elongate and slightly crescent shaped NW lateral shoreline of SLE, this results in the grounded ice to the
205 NNE of the trough becoming afloat not at the narrow up-ice end of the lake, but instead across a much
206 greater length of shoreline at the NE edge of the lake. Consequently, englacial layer drawdown, possibly

207 associated with lake shoreline melting (Siegert and others, 2000, 2004; Tikku et al., 2005), is not confined
208 just to the narrow (<1.5 km) up-ice tip of the lake shoreline, as it would be if ice flow was directly along
209 the trough and lake axis, but instead occurs along a shoreline of 5 km.

210 It is possible that alternative factors may contribute to the geometry of the internal layers over and
211 around the lake. These include the significant relief (>2 km) between the floor of the Ellsworth Trough and
212 the high elevation topography surrounding it, and the shift at the lake shoreline from a no-slip bed to a bed
213 with zero basal resistance (Weertman, 1976). Combined with the oblique ice flow direction, the drawdown
214 of the internal layering may at least partly be a result of mechanical effects of ice flow off the subglacial
215 high and into the deep trough, combined with the ‘Weertman effect’. Disentangling the relative importance
216 of basal melt vs. sliding/no-sliding transitions vs. mechanical effects with detailed 3D numerical modelling
217 is beyond the scope of this paper, however. Instead, we assess the vertical and spatial patterns of englacial
218 layer drawdown, comparing our observations with existing numerical models that predict: (a) 3D flow
219 influences on englacial layering (Leysinger Vieli and others, 2007); and (b) water circulation and basal
220 mass balance within SLE (Woodward and others, 2010; Thoma and others, 2011). We also evaluate the
221 limitations of the SLE englacial layers dataset and discuss the implications of layer drawdown patterns for
222 sediment deposition in the lake.

223 Despite the 3D complexity of the ice flow over and around SLE, we suggest that it may be possible
224 to identify the separate effects of both the Weertman effect and basal melt on the SLE layers. There is
225 substantial drawdown of englacial layers in the upper 50-60% of the ice column (i.e. between layer picks
226 3-6, Figures 2c and 3d-g) NW of the lake. This layer drawdown may be the result of the transition from
227 no-sliding to sliding as the ice flows over the lake, combined with the impact of ice flow off the high relief
228 subglacial topography (Figure 1c). In contrast, the greatest amplitude of layer drawdown in layers 7 and 8
229 (Figures 2c and 3h) is over the NW half of the lake. This SE-ward shift in the maximum amplitude of layer
230 drawdown with ice thickness could be the result of basal melting over the lake becoming the dominant
231 influence on englacial stratigraphy as the ice sheet flows down, and slightly across, the lake. This spatial
232 and vertical pattern of drawdown is consistent with numerical modelling of 3D layer form (Leysinger Vieli
233 and others, 2007), which suggests that the amplitude of layer drawdown is greater higher up the ice column
234 (in response to sliding) than for the basal melt case (which has greatest drawdown amplitude near to the
235 bed).

236 The drawdown of the deepest englacial layers over SLE (i.e. layers 7 and 8) has an apparent spatial

237 consistency with the pattern of basal mass balance derived from numerical modelling of water circulation
238 in the lake (Figure 3 of Woodward and others, 2010). Using an idealised lake geometry, and assuming a
239 closed system, this modelling suggested very high basal melting of 16 cm a^{-1} in a linear localised zone
240 proximal to the grid-NW side of SLE (Figure 3 of Woodward and others, 2010). This rate is 2-4 times
241 greater than the melt rate over the centre of the lake, and elsewhere in the up-ice half of the lake. The
242 apparent spatial correspondence between this pattern of modelled melting (Woodward and others, 2010)
243 and the englacial layer drawdown reported here, suggests that the water circulation model produces a
244 relatively realistic representation of the pattern of melting across the lake.

245 It is important to recognise the limitations of the SLE layers dataset. It is by no means a perfect
246 and comprehensive dataset, and its complexity has potential implications for our ability to confidently
247 evaluate the relative influence of basal melt and changes in basal sliding over the lake. First, englacial
248 layers are only imaged and picked in the radar data for the upper 2/3rds of the ice column (Figure 2).
249 Numerical modelling (Leysinger Vieli and others, 2007), albeit assuming a flat bed, suggests that the effects
250 of basal melting will cause the largest amplitude of layer drawdown at the base of the ice column, whereas
251 the greatest impact of the Weertman effect will be found in layers at ice thicknesses of approximately
252 2/3rds. The radar data do not image layers at depth over SLE, however, limiting their use in identifying
253 zones of basal melt. Second, the SLE radar survey (Figure 1a) was designed primarily for mapping the
254 extent of the lake and its subglacial hydrological catchment. However, this design was not optimised for
255 characterisation of englacial layering as the survey grid (Figure 1a) and the 'along flow' radar lines (e.g.
256 Figure 2b) are typically oblique to ice flow (Figure 1b). The complex relationship between ice flow and the
257 survey lines further complicates our ability to fully disentangle basal melting from the Weertman effect.
258 Third, the englacial structure is further complicated by localised folding caused by ice flow over rugged
259 subglacial topography (Ross and others, 2011b) (Figure 2a). These folds, which track obliquely across the
260 lake, disrupt the radar stratigraphy and make it difficult to confidently pick contiguous stratigraphic layers
261 (Figure 2c). This is the case even for radar profiles that are oriented closer to 'along flow' (e.g. Figure 2b),
262 due to the oblique tracking of the fold axes (Figure 2d).

263 The geometry of the englacial layering, combined with the basal mass balance output from the water
264 circulation modelling, has potential implications for the pattern and rate of sediment deposition in SLE. The
265 2D conceptual models produced to date (Bentley and others, 2011; Smith and others, 2018) have neglected
266 the 3D implications of layer drawdown along the long grid-NW shoreline of the lake and basal melt being

267 focused on the NW side of the lake. Instead they assume a relatively constant rate of rainout from the
268 ice column across the up-ice parts of the lake, focused on the narrower up-valley (i.e. NE) grounding
269 zone. The englacial layers and the modelling instead point to a possibly more targeted pattern of sediment
270 rainout from the ice base, with greater flux of sediment likely above the parts of the lake more proximal
271 to the longer grid-NW shoreline. Whether all rained-out sediment is deposited directly without further
272 transport via overflows or underflows in the lake is unknown at present, and is theoretically complicated by
273 the presence of the Line of Maximum Density within the lake (Woodward and others, 2010; Bentley and
274 others, 2011; Pattyn and others, 2016). However, we can assume that coarser material will be deposited
275 directly by gravity, meaning that greater rates of sediment deposition are possible beneath the zone of
276 significant englacial layer drawdown, and that there is the potential for occasional coarser material to be
277 present nearer to the proposed access location (Woodward and others, 2010) than previously considered.
278 Low acoustic impedance values, indicating a clay- to silt-rich matrix, dominate the lake floor sediments,
279 however, indicating that fine-grained material is abundant across the lake floor (Smith and others, 2018).

280 The DEM and derived hydropotential of the SLE outlet zone further emphasises the geomorphic and
281 structural geological controls on the location, extent and geometry of SLE (Ross and others, 2014), and
282 most likely other subglacial lakes in the Ellsworth Subglacial Highlands (Vaughan and others, 2007; Rivera
283 and others, 2015). They also hint at geomorphic evidence for hydrological connections between lakes in
284 the region. It is clear from RES evidence that there is abundant subglacial water within the catchment
285 both up and down ice of SLE (e.g. Figure 4). As such, hydraulic connectivity, even if only episodic, is a
286 distinct possibility, particularly over glacial-interglacial cycles, when ice divide migration may occur, with
287 potential implications for ice surface slope gradients. Any changes in ice-flow configuration (e.g. from ice
288 divide migration over geological timescales) could also lead to variability in the location, rate and pattern
289 of sediment influx and deposition into SLE by altering the distribution and pattern of basal melting. Such
290 changes are unlikely to have occurred over the Holocene, however (Ross and others, 2011b). The chemistry
291 of water emanating from melted ice directly over the lake will be distinct from that derived from the
292 upstream lake (Figure 4), given the opportunity for solute acquisition when in contact with basal sediment
293 during basal water flow from one lake to the other. This may also vary over time.

294 One aspect that our current dataset does not allow us to evaluate is the relative importance of basal
295 melt or the input of water into SLE from these subglacial hydrological pathways. However, our study does
296 demonstrate the potential variability in the spatial pattern of basal melting across the lake. Were future

297 investigations of subglacial lakes in areas of significant subglacial relief (e.g. Lago CECs or SLE) to attempt
298 to determine basal melt rates (e.g. using ApRES), then those investigations cannot assume that basal melt
299 rates will be greatest over the centre of the water body or at the top end of the lake. As such, detailed
300 characterisation of the geometry of englacial layers over target lakes is necessary prior to site selection for
301 measurements of basal melt.

302 CONCLUSIONS

- 303 1. We characterise the geometry of englacial layers over and around Subglacial Lake Ellsworth (SLE) using
304 low frequency RES data.
- 305 2. Englacial layers are drawn down in a zone that is located along the grid NW shoreline of SLE, and over
306 the NW half of the lake.
- 307 3. Layer drawdown is interpreted to be the result of: (a) the Weertman effect along the length of the
308 ‘grounding line’ of the lake’s grid-NW shoreline caused by ice flow oblique to the lake; and (b) a zone
309 of enhanced basal melt above the NW half of the lake. However, we cannot also entirely rule out the
310 influence of mechanical effects associated with significant subglacial relief.
- 311 4. The pattern of drawdown inferred from the englacial layers directly over the lake is spatially consistent
312 with basal mass balance output from a previously published model of water circulation in SLE.
- 313 5. Layer drawdown and basal melt over the NW half of the lake has implications for the rate and pattern
314 of sedimentation in SLE, and for future measurement and modelling of basal melting over subglacial
315 lakes.
- 316 6. Our data do not permit us to determine the relative importance of basal melting compared to inputs from
317 subglacial water. However, the RES data and derived products (e.g. DEMs and maps of hydropotential),
318 do suggest that hydrological connectivity of the cascade of lakes within the Ellsworth Trough is possible,
319 at least episodically. Both direct basal melting (i.e. over the lake), and basal hydrological inputs from
320 the wider catchment will influence physical conditions within SLE.
- 321 7. No current evidence exists for the presence of englacial reflections associated with accretion ice over
322 SLE.

323 **ACKNOWLEDGEMENTS**

324 This work was funded by Natural Environment Research Council (NERC) Antarctic Funding Initiative
325 (AFI) grants NE/D008751/1, NE/D009200/1, and NE/D008638/1. We thank the British Antarctic Survey
326 for logistics support, NERC Geophysical Equipment Facility for equipment (loans 838, 870), and Dan
327 Fitzgerald and Dave Routledge for excellent field work support. We are grateful to Richard Hindmarsh
328 for productive discussions on the likely processes influencing englacial layer geometry over Subglacial Lake
329 Ellsworth, Ed King for the emergency loan of his DELORES1 radar in the 07/08 field season season, and
330 to Hugh Corr and Mark Maltby for the design and build of DELORES2. John Woodward and Andy Smith
331 are thanked for their support, guidance and readings of the poetry of William McGonagall during the
332 07/08 SLE field season. Knut Christianson (Scientific Editor), Gwendolyn Leysinger-Vieli and a second
333 anonymous reviewer are thanked for their helpful, supportive and constructive reviews that considerably
334 improved the paper. Aspects of this work were inspired and motivated by the Scientific Committee for
335 Antarctic Research (SCAR) AntArchitecture community.

336 **DATA AVAILABILITY**

337 Shapefiles and gridded surfaces of the picked englacial layers will be made available via the Newcastle
338 University research data repository (<https://data.ncl.ac.uk/>) in due course.

339 **REFERENCES**

- 340 Barcilon, V, and MacAyeal, D (1993) Steady flow of a viscous ice stream across a no-slip/free-slip
341 transition at the bed. *Journal of Glaciology*, 389, 167-185.
- 342 Bell, RE, Studinger, M, Tikku, AA, Clarke, GKC, Gutner, MM and Meertens, C (2002) Origin and
343 fate of Lake Vostok water frozen to the base of the East Antarctic ice sheet. *Nature*, 416, 307-310.
- 344 Bentley, MJ, Christoffersen, P, Hodgson, DA, Smith, AM, Tulaczyk, A and Le Brocq, AM (2011)
345 Subglacial Lake Sediments and Sedimentary Processes: Potential Archives of Ice Sheet Evolution,
346 Past Environmental Change, and the Presence of Life. In: M.J. Siegert, M.C. Kennicutt II, and R.A.
347 Bindschadler, ed. *Antarctic Subglacial Aquatic Environments*. Washington, D.C: AGU, pp.83-110.
- 348 Carter, SP, Blankenship, DD, Young, DA and Holt, JW (2009) Using radar-sounding data to identify

349 the distribution and sources of subglacial water: application to Dome C, East Antarctica. *Journal of*
350 *Glaciology*, 55, 1025-1040.

351 Dowdeswell, JA and Evans, S (2004) Investigations of the form and flow of ice sheets and glaciers
352 using radio-echo sounding. *Reports on Progress in Physics*, 67, 1821-1861.

353 Drewry, DJ and Meldum, DT (1978) Antarctic airborne radio echo sounding, 1977–78. *Polar Record*,
354 19, 267-273.

355 Fricker, HA, Scambos, T, Bindschadler, R and Padman, L, (2007) An Active Subglacial Water System
356 in West Antarctica Mapped from Space. *Science*, 315, 1544-1548.

357 Fricker, HA, Siegfried, MR, Carter, SP and Scambos, TA (2016) A decade of progress in observing
358 and modelling Antarctic subglacial water systems. *Philosophical Transactions of the Royal Society*,
359 374, 20140294.

360 Gudlaugsson, E, Humbert, A, Kleiner, T, Kohler, J and Andreassen, K (2016) The influence of a
361 model subglacial lake on ice dynamics and internal layering. *The Cryosphere*, 10, 751-760.

362 Howat, IM, Porter, C, Smith, BE, Noh, MJ and Morin, P (2019) The Reference Elevation Model of
363 Antarctica. *The Cryosphere*, 13, 665-674.

364 Hutchinson, MF (1988) Calculation of hydrologically sound digital elevation models, in *Proceedings:*
365 *Third International Symposium on Spatial Data Handling*, 117–133, International Geographic Union,
366 Commission on Geographic Data Sensing and Processing, Columbus, Ohio, 17–19 August 1988.

367 Jeofry, H, Ross, N, Corr, HFJ, Li, J, Morlighem, M, Gogineni, P and Siegert, MJ (2018) A new bed
368 elevation model for the Weddell Sea sector of the West Antarctic Ice Sheet. *Earth System Science*
369 *Data*, 10, 711–725.

370 Jordan, TA, Martin, C, Ferraccioli, F, Matsuoka, K, Corr, H, Forsberg, R, Olesen, A and Siegert, M
371 (2018) Anomalously high geothermal flux near the South Pole. *Scientific Reports*, 8, 16785.

372 King, EC, Pritchard, HD and Smith, AM (2016) Subglacial landforms beneath Rutford Ice Stream,
373 Antarctica: detailed bed topography from ice-penetrating radar. *Earth System Science Data*, 8,
374 151-158.

375 Leonard, K, Bell, RE, Studinger, M and Tremblay, B (2004) Anomalous accumulation rates in the
376 Vostok ice-core resulting from ice flow over Lake Vostok. *Geophysical Research Letters*, 31, L24401,
377 doi:10.1029/2004GL021102.

378 Leysinger Vieli, GJ-MC, Hindmarsh, RCA, and Siegert, MJ (2007) Three-dimensional flow influences
379 on radar layer stratigraphy. *Annals of Glaciology*, 46, 22-28.

380 Mayer, C, Grosfeld, K and Siegert, MJ (2003) The effect of salinity on water circulation within
381 subglacial Lake Vostok. *Geophysical Research Letters*, 30, doi 10.1029/2003GL017380.

382 Mouginot, J, Rignot, E and Scheuchl, B (2019) MEaSURES Phase-Based Antarctica Ice Velocity
383 Map, Version 1. doi: <https://doi.org/10.5067/PZ3NJ5RXHRH10>.

384 Pattyn, F, Carter, SP and Thoma, M (2016) Advances in modelling subglacial lakes and their inter-
385 action with the Antarctic ice sheet. *Philosophical Transactions of the Royal Society A* 374: 20140296.
386 <http://dx.doi.org/10.1098/rsta.2014.0296>

387 Rivera, A, Uribe, J, Zamora, R and Oberreuter, J (2015) Subglacial Lake CECs: Discovery and
388 in situ survey of a privileged research site in West Antarctica. *Geophysical Research Letters*, 42,
389 3944–3953.

390 Ross, N, Siegert, MJ, Rivera, A, Bentley, MJ, Blake, D, Capper, L, Clarke, R, Cockell, CS, Corr,
391 HFJ, Harris, W, Hill, C, Hindmarsh, RCA, Hodgson, DA, King, EC, Lamb, H, Maher, B, Makinson,
392 K, Mowlem, M, Parnell, J, Pearce, DA, Priscu, J, Smith, AM, Tait, A, Tranter, M, Wadham, JL,
393 Whalley, WB and Woodward, J (2011) Ellsworth Subglacial Lake, West Antarctica: A review of its
394 history and recent field campaigns. In: M.J. Siegert, M.C. Kennicutt II, and R.A. Bindschadler, ed.
395 *Antarctic Subglacial Aquatic Environments*. Washington, D.C: AGU, pp.221-233.

396 Ross, N, Siegert, MJ, Woodward, J, Smith, AM, Corr, HFJ, Bentley, MJ, Hindmarsh, RCA, King,
397 EC and Rivera, A (2011b) Holocene stability of the Amundsen-Weddell ice divide, West Antarctica.
398 *Geology*, 39, 935-938.

399 Ross, N, Jordan, TA, Bingham RG, Corr, HFJ, Ferraccioli, F, Le Brocq, A, Rippin, DM, Wright,
400 AP and Siegert, MJ (2014) The Ellsworth Subglacial Highlands: inception and retreat of the West
401 Antarctic Ice Sheet. *Geological Society of America Bulletin*, 126, 3-15.

- 402 Siegert, MJ (1999) On the origin, nature and uses of Antarctic ice-sheet radio-echo layering. Progress
403 in Physical Geography, 23, 159-179.
- 404 Siegert, MJ (2005) LAKES BENEATH THE ICE SHEET: The Occurrence, Analysis, and Future
405 Exploration of Lake Vostok and Other Antarctic Subglacial Lakes. Annual Reviews of Earth and
406 Planetary Science, 33, 215-245.
- 407 Siegert, MJ, Kwok, R, Mayer, C and Hubbard, B (2000) Water exchange between the subglacial Lake
408 Vostok and the overlying ice sheet. Nature, 403, 643-646.
- 409 Siegert, MJ, Hindmarsh, R, Corr, H, Smith, A, Woodward, J, King, EC, Payne, AJ and Joughin, I
410 (2004) Subglacial Lake Ellsworth: A candidate for in situ exploration in West Antarctica. Geophysical
411 Research Letters, 31, L23403, doi:10.1029/2004GL021477.
- 412 Siegert, MJ, Clarke, RJ, Mowlem, M, Ross, N, Hill, CS, Tait, A, Hodgson, D, Parnell, J, Tranter,
413 M, Pearce, D, Bentley, MJ, Cockell, C, Tsalogou, M-N, Smith, A, Woodward, J, Brito, MP and
414 Waugh, E (2012) Clean access, measurement and sampling of Ellsworth Subglacial Lake: A method
415 for exploring deep Antarctic subglacial lake environment. Reviews of Geophysics, 50, RG1003.
- 416 Siegert, MJ, Makinson, K, Blake, D, Mowlem, M and Ross, N (2014) An assessment of deep hot-
417 water drilling as a means to undertake direct measurement and sampling of Antarctic subglacial lakes:
418 experience and lessons learned from the Lake Ellsworth field season 2012-13. Annals of Glaciology,
419 55, 59-73.
- 420 Smith, A, Woodward, J, Ross, N, Bentley, MJ, Hodgson, DA, Siegert, MJ and King, EC (2018)
421 Evidence for the long-term sedimentary environment in an Antarctic subglacial lake. Earth and
422 Planetary Science Letters, 504, 139-151.
- 423 Thoma, M, Grosfeld, K and Mayer, C (2008a) Modelling accreted ice in subglacial Lake Vostok,
424 Antarctica. Geophysical Research Letters, 35, L11504, doi:10.1029/2008GL033607.
- 425 Thoma, M, Mayer, C and Grosfeld, K (2008b) Sensitivity of subglacial Lake Vostok's flow regime on
426 environmental parameters, Earth and Planetary Science Letters, 269, 242-247.
- 427 Thoma, M, Grosfeld, K, Filina, I and Mayer, C (2009) Modelling flow and accreted ice in subglacial
428 Lake Concordia, Antarctica. Earth and Planetary Science Letters, 286, 278-284.

- 429 Thoma, M, Grosfeld, K, Mayer, C, Smith, AM, Woodward, J and Ross, N (2011) The "tipping"
430 temperature within Subglacial Lake Ellsworth, West Antarctica and its implications for lake access.
431 *The Cryosphere*, 5, 561-567.
- 432 Tikku, AA, Bell, RE, Studinger, M, Clarke, GKC, Tabacco, I and Ferraccioli, F (2005) Influx of
433 meltwater to subglacial Lake Concordia, East Antarctica. *Journal of Glaciology*, 51, 96-104.
- 434 Vaughan, DG, Rivera, A, Woodward, J, Corr, HFJ, Wendt, J and Zamora, R (2007). Topographic
435 and hydrological controls on Subglacial Lake Ellsworth, West Antarctica. *Geophysical Research*
436 *Letters*, 34, L18501, doi:10.1029/2007GL030769.
- 437 Wingham, DJ, Siegert, MJ, Shepherd, AP, and Muir, AS (2006) Rapid discharge connects Antarctic
438 subglacial lakes. *Nature*, 440, 1033-1036.
- 439 Woodward, J, Smith, AM, Ross, N, Thoma, M, Corr, HFJ, King, EC, King, MA, Grosfeld, K, Tranter,
440 M and Siegert, MJ (2010) Location for direct access to subglacial Lake Ellsworth: An assessment of
441 geophysical data and modeling. *Geophysical Research Letters*, 37(11), L11501.
- 442 Wright, AP, Young, DA, Roberts, JL, Schroeder, DM, Bamber, JL, Dowdeswell, JA, Young, NW,
443 Le Brocq, AM, Warner, RC, Payne, AJ, Blankenship, DD, van Ommen, TD and Siegert, MJ (2012)
444 Evidence of a hydrological connection between the ice divide and ice sheet margin in the Aurora Sub-
445 glacial Basin, East Antarctica. *Journal of Geophysical Research*, 117, F01033, doi:10.1029/2011JF002066.
- 446 Wüest, A and Carmack, E (2000) A priori estimates of mixing and circulation in the hard-to-reach
447 water body of Lake Vostok. *Ocean Modelling*, 2, 29–43.